J Electroceram (2011) 27:203–208
DOI 10.1007/s10832-011-9666-3

Effects of temperature on structural and optical properties of ZnMgO films fabricated by pulsed laser deposition

Yong-Jie Wang · Xian-Qi Wei · Ran-Ran Zhao · Chuan-Song Chen · Shang Gao · Jie Lian

Received: 18 May 2011 / Accepted: 8 November 2011 / Published online: 19 November 2011

Abstract ZnMgO thin films have been deposited on Si (111) substrates by pulsed laser deposition (PLD) technique at growth temperature from 300 to 700°C in nitrogen ambient of 1.0 Pa. The effects of growth temperature on structural and optical properties of deposited ZnMgO thin films have been characterized by X-ray diffraction (XRD), scanning electron microscopy (SEM), infrared absorption (IR) spectra and photoluminescence (PL) spectra. The results of XRD and SEM analyses show that the film fabricated at 400°C possesses good crystallinity with hexagonal wurtzite structure and surface morphology. The Mg has been incorporated into ZnO in the form of substitutional Zn. The IR spectra reveal the typical absorption peaks of ZnMgO. The band-gap values have been obtained from 2.96 to 4.23 eV with increasing growth temperature. The PL spectra show that the highest UV emission is obtained at growth temperature of 600°C, and the obvious blue-shift is observed. This may be assigned as the change of the band-gap due to the increasing incorporation of Mg^{2+} ions with the increasing growth temperature.

Y.-J. Wang · X.-Q. Wei (✉) · R.-R. Zhao
School of Physics and Technology, University of Jinan,
Jinan 250022, People's Republic of China
e-mail: xqwei666@sohu.com

C.-S. Chen
College of Physics and Electronics, Shandong Normal University,
Jinan 250014, People's Republic of China

S. Gao · J. Lian
School of Information Science and Engineering,
Shandong University,
Jinan 250100, People's Republic of China

Keywords PLD · ZnMgO thin films · Crystal structure · Band-gap · Optical properties

1 Introduction

Zinc oxide (ZnO), as a kind of semiconductor oxide, has caused extensive attention due to the wide band-gap (3.37 eV at room temperature) and the large exciton binding energy (60 meV). ZnO is widely used in short-wavelength optic-electronic devices, such as solar cell, ultraviolet (UV) laser, liquid crystal display [1–3], etc. The band-gap width of ZnO can be increased by alloying, and magnesium oxide (MgO) is usually employed as a promising material. ZnMgO alloy is generally formed when Zn^{2+} in ZnO are partially replaced by Mg^{2+}. In addition, the similar radii of Mg^{2+} (0.57 Å) and Zn^{2+} (0.60 Å) [4] avoid the formation of high-density defects resulting from the stress mismatch. As a ternary semiconductor compound, ZnMgO has a larger band-gap than ZnO. Due to the different proportion of Mg doped, the band-gap width of ternary ZnMgO can be changed in 3.37–7.8 eV [5]. According to the phase diagram of the ZnO–MgO system, the thermodynamic solid solubility of MgO in ZnO is less than 4 mol%. But by using some certain fabrication techniques such as PLD, the solubility can be improved to 33 mol% [6] in ZnMgO thin films. Some reports showed that Mg content in ZnMgO reaches 49 mol% by molecular beam epitaxy (MBE) [7] and metal-organic vapor-phase epitaxy (MOVPE) [8] techniques. As the increasing proportion of Mg, the structure of ZnMgO can be changed from hexagonal to cubic phase [3, 9]. Most studies demonstrate that the band-gap of ZnMgO can be remarkably increased by changing the proportion of doped Mg content. However, few profound works about effect of growth temperature on

band-gap of ZnMgO thin films fabricated on Si(111) substrates in N_2 ambient were reported.

Recently, several different deposition techniques have been used to prepare ZnMgO thin films, such as thermal evaporation [10], magnetron sputtering [11], MBE [12], MOVPE [13], microwave assisted combustion (MAC) synthesis [14] and PLD [15]. Among these techniques, PLD has become an important technique to fabricate high quality thin films at low temperature, especially for improving the stoichiometry of ZnMgO thin films with increasing fabrication temperature. In this paper, ZnMgO films were fabricated on Si(111) substrates at different temperature in N_2 ambient by using PLD technique. The structural, optical properties and the change of band-gap of ZnMgO thin films were systematically studied.

2 Experiment

ZnMgO thin films were fabricated on Si(111) substrates by PLD at substrate temperature from 300 to 700°C. The deposition process was carried out in a stainless steel vacuum chamber evacuated to a base pressure of 5.0×10^{-5} Pa by a turbomolecular pump. A KrF excimer laser with a wavelength of 248 nm (the repetition is 10 Hz and the duration is 25 ns) was focused by a lens on the target at an incidence angle of 45°. The target with a diameter of 25 mm was prepared by mixing ZnO and MgO powders with the molar ratios of 9:1, and then sintered at 100°C for 1 h, 550°C for 3 h and 1000°C for 12 h, respectively. The Si substrates were cleaned several times with ultrasonic vibration in ethanol and high purity water before depositing. The target-substrate distance was kept at 40 mm. The target and the substrates were rotated reversely at 6 rpm. The deposition time was 15 min. During deposition, N_2 was used as background gas, and the pressure was fixed at 1.0 Pa by adjusting the flow rate of the N_2 gas. The laser incident energy was kept at 200 mJ/pulse.

The structural properties of ZnMgO thin films were characterized by D8-advance type X-ray diffractometer with Cu Kα-source (λ=0.1541 nm). The surface morphology and the microstructure were studied using field emission scanning electron microscopy (FESEM) (QUANTA 250). Mg content and EDX spectra were investigated by energy dispersive X-ray spectroscopy. France SOPRA GES-5 type spectroscopic ellipsometer was used to measure the thicknesses and optical parameters of the ZnMgO thin films. The IR spectra were carried out by employing the BRUKER TENSOR27 spectrophotometer (wavenumber range is 400–4,000 cm^{-1}, optical resolution is 4 cm^{-1}) in transmission mode. The PL spectra were measured by using PERKINELMERLS55 fluorescence spectrometer with the excitation wavelength of 325 nm pumped by a high energy pulsed Xe source.

3 Results and discussion

3.1 Structural properties

Figure 1 shows the XRD patterns of ZnMgO thin films deposited on Si substrates at different temperature from 300 to 700°C in N_2 ambient, the enlarged XRD pattern for ZnMgO fabricated at 500°C is shown in the insert. Figure 1 (a) and (b) present the (002) diffraction peak of ZnMgO thin films fabricated at 300–400°C. Only the (002) peak appears in ZnMgO thin films fabricated at 300 and 400°C, indicating these films are preferred c-axis orientation with hexagonal structure. The (002) peak and a negligible cubic ZnMgO(200) peak located at 42.54° are observed in Fig. 1 (c) for ZnMgO film deposited at 500°C. It is an indication that the Mg^{2+} ions successfully substitute the Zn^{2+} ions sites in ZnMgO thin film with the increasing deposition temperature. In addition, the coexistence of hexagonal and cubic phases demonstrates that the structure of ZnMgO films begin to transform from wurtzite to rock-salt-cubic structure. The increase of substituted Mg in crystal may be the reason of the transformation [15]. When the Mg and Zn atoms bond to O atom, the Mg atom is easier to lose electrons than Zn atom due to the different Pauling electronegativities (Mg is 1.31, Zn is 1.65), resulting in the increase of the quantity of Mg–O bond. Only ZnMgO (200) peak located at 42.54° can be observed for ZnMgO film deposited at 600°C. It has a slight deviation towards low angle compared with 2θ value of MgO(200) diffraction peak (42.98°), indicating that most of Zn^{2+} ions have been substituted by Mg^{2+} ions.

The intensity of the (002) peaks of ZnMgO thin films increases with the increasing growth temperature until 400°C,

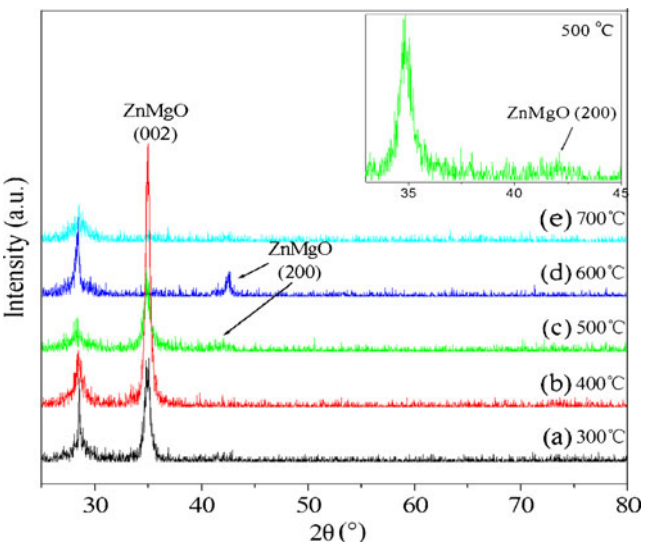

Fig. 1 XRD patterns of ZnMgO films deposited on Si substrate at various temperature from 300–700°C

then decreases at 500°C and disappears at 600 and 700°C. The full-width at half-maximum (FWHM) values of (002)peak and average crystallite size of the thin films prepared at different temperature are shown in Table 1. The average crystallite size is calculated by using Scherrer's formula [16]. The minimal FWHM and the intense peak are obtained at 400°C, indicating the best crystalline quality of ZnMgO thin film. The film deposited at 700°C is amorphous as shown in Fig. 1(e), indicating that it is unfavorable for the growth of ZnMgO thin films at the high growth temperature in PLD system. The reason is that the re-evaporation of particles on the surface of thin films is high at 700°C so that the crystalline quality of the films is deteriorated.

The SEM photographs, nano-structure image and EDX spectrum of ZnMgO thin films are shown in Fig. 2. The SEM photographs in Fig. 2(a–e) present that the quality of the films are improving from 300 to 400°C and then becomes deteriorative with increasing growth temperature. As growth temperature is from 300 to 400°C, the average grain size increases and the distribution of grain orientation is more alignment. The most smooth and compact surface of the film is obtained at 400°C. When the temperature is 500, 600 and 700°C, the surface coarseness of ZnMgO thin films is increasing, and the crystalline grains are decreasing as shown in Fig. 2(c–e). The results are consistent with XRD observations. As analysed by XRD, the structure of ZnMgO changes from wurtzite structure to rock-salt-cubic structure at high growth temperature. Figure 2(f) is the nano-structure derived from ZnMgO thin film fabricated at 400°C. Occasionally, we can also find some claval structure of ZnMgO with the hexagonal wurtzite structure as marked in Fig. 2(f). Figure 2(g) shows the EDX spectrum derived from the sample in Fig. 2(b). The O, Mg, Zn, Si peaks can be observed, indicating that ZnMgO films are fabricated on Si(111) substrates successfully.

The atomic concentration of Mg composition of ZnMgO thin films deposited at different temperatures is given in Table 1. The values of the concentration values are given directly from the EDX experimental date. It can be seen that the atomic concentration of Mg composition increases from 30 at.% to 39 at.% with the increase of the temperature from 300 to 700°C. The Mg content values in ZnMgO thin films are higher than that in the target in this study. The phenomena may be appeared in some fabricated techniques such as PLD, magnetron sputtering etc. [8, 17]. Zhang et al. reported the growth of ZnMgO thin film by using ZnMgO ceramic target with Mg:Zn(1:1) atomic ratio, and obtained the ZnMgO thin film with Mg containing 70 at.% by magnetron sputtering [18]. Generally, the vapour pressure of Zn is higher than that of Mg, which leads to the desorption of Zn-related species and the condensation of Mg-related species on the substrate. Therefore, the Mg content in ZnMgO film can be increased easily than that of Zn with increasing growth temperature in PLD system. However, the increase of re-evaporation of particles on the surface of thin films in higher temperature results in the decrease of film thickness. The elimination of some defects formed at deposition process in high deposited temperature such as Zn interstitial and O vacancy, especially vacancies in thin films can also result in the decrease of thickness of ZnMgO thin films. The variation of thicknesses of ZnMgO thin films as a function of deposited temperatures is shown in Table 1.

3.2 Optical properties

The absorption properties of ZnMgO thin films were measured by using spectroscopic ellipsometer. The direct optical band-gap (Eg) of ZnMgO thin films can be determined by the relationship between the absorption coefficient α and the photon energy ($h\nu$) using the formulas as follows.

$$\alpha h\nu = C(h\nu - Eg)^{1/2} \quad (1)$$

$$\alpha = 4\pi k/\lambda \quad (2)$$

where C is a constant of the direct transitions, k is extinction coefficient, which can be given by measurement of spectroscopic ellipsometer, and λ is incident wavelength. Figure 3(a) shows the variation of extinction coefficient k as a function of wavelength λ. Figure 3(b) shows the variation of $(\alpha h\nu)^2$ versus $h\nu$ for ZnMgO films. The optical band gap Eg of ZnMgO films is obtained by extrapolating the straight line portion to the energy axis [19]. The Eg values can be determined to be 2.96, 3.44, 3.84, 4.05, 4.23 eV with increasing growth temperature, respectively. The results illustrate that the optical band gaps are

Table 1 Mg composition and the thicknesses of ZnMgO thin films fabricated at different temperatures

Temperature (°C)	FWHM (°)	Grain size (nm)	Mg composition (at %)	Thickness (nm)
300	0.55934	25	30±4	131
400	0.45268	31	30±8	108
500	0.65781	21	35±3	99
600	–	–	38±3	66
700	–	–	39±4	32

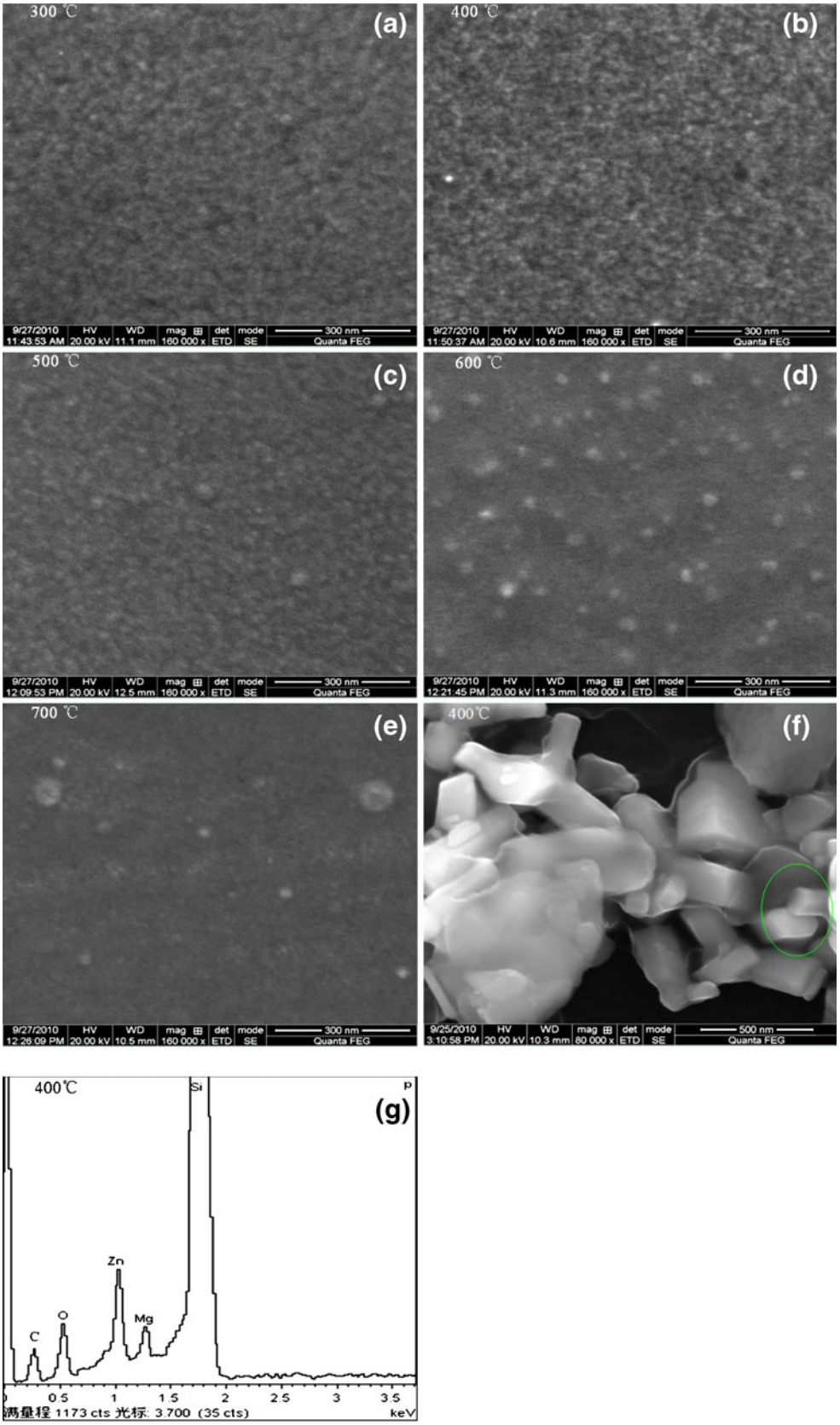

Fig. 2 (**a**–**e**) SEM photographs of ZnMgO samples at different temperature. (**f**) Nanostructure of ZnMgO thin film. (**g**) EDX spectrum of ZnMgO film grown at 400°C

increasing in ZnMgO thin films with the increasing temperature from 300 to 700°C.

The absorption of infrared is a result to bring about some different energy bands in a molecular to stretch and bend

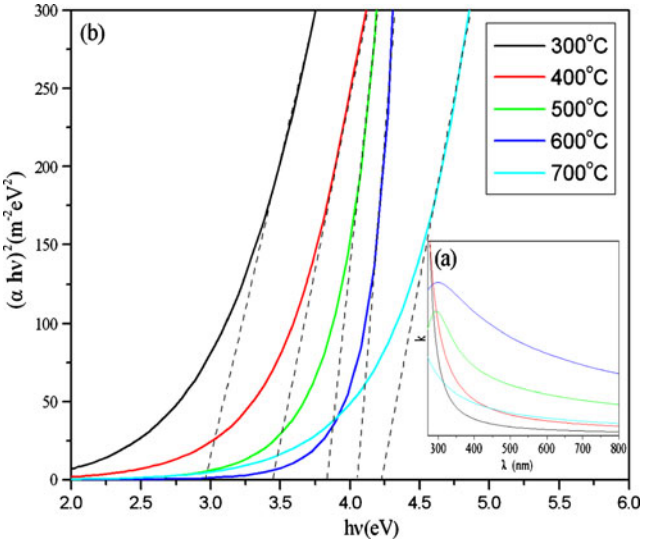

Fig. 3 (**a**) The relationship between extinction coefficient(k) and wavelength(λ). (**b**) $(\alpha h\nu)^2$ versus photon energy ($h\nu$) of ZnMgO films deposited at the temperature form 300 to 700°C

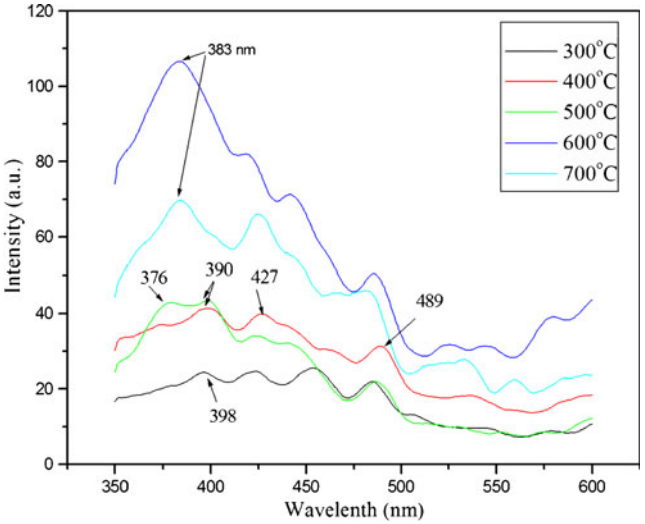

Fig. 5 Rome temperature PL spectra of ZnMgO films deposited on Si substrates at different growth temperature

with respect to one another [20]. The infrared spectra of ZnMgO thin films fabricated at the temperature from 300 to 700°C and the amplification image of typical peak are given in Fig. 4(a) and (b), respectively. The spectra contain three main absorption bands located at wavenumbers 418, 608 and 1,109 cm^{-1}. The absorption band at 418 cm^{-1} is the typical absorption band of ZnMgO attributed to the bending vibration absorption of Zn–Mg–O bond. The band at 608 cm^{-1} is caused by local vibration of substitutional carbon in Si crystal lattice [21], and 1,109 cm^{-1} is vibration absorption of Si–O bond [22]. As shown in Fig. 4 (b), the intensity and width of IR spectra peak located at 418 cm^{-1} of ZnMgO films are increasing with increasing growth

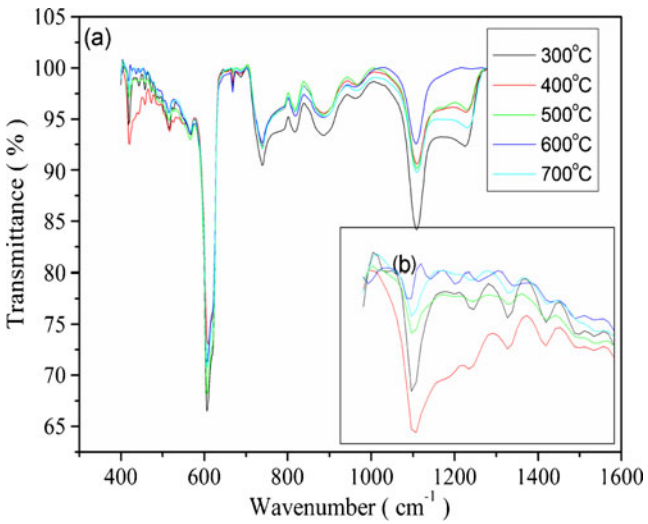

Fig. 4 (**a**) IR absorption spectra of ZnMgO thin films fabricated at different temperature. (**b**) The amplification of typical peak sited at 418.18 cm^{-1}

temperature. The absorption band at 418 cm^{-1} for ZnMgO thin film fabricated at 400°C is the strongest. However, compared with the IR spectrum of ZnO [23], the intensity of the typical peak is weak. This may be the effect of substitutional Mg^{2+} causing the decrease of vibration absorption of Zn–Mg–O bond.

Figure 5 shows the room temperature PL spectra of ZnMgO thin films fabricated on Si(111) substrates at different temperature from 300 to 700°C. PL spectra show the UV emission band at 377–399 nm and a weaker visible emission. The UV emission is near-band-edge emission (NBE), caused by the exiton recombination [24]. The intensity of the UV emission peak increases gradually up to 600°C. When the temperature is over 600°C, the decrease of the UV emission intensity is attributed to the re-evaporation of adatoms and the decreasing Mg content. It can be seen from the PL spectra that the UV emission peak has an obvious blue shift from 398 to 383 nm for ZnMgO thin films deposited from 300 to 700°C. This is an indication of the band-gap broadening with Mg doping into ZnO. Two peaks located at 398 and 383 nm appear in the UV emission band for ZnMgO thin films deposited at 500°C. Combined with the analysis of XRD spectrum at 500°C, it may be related to the appearance of (002) peaks both ZnMgO hexagonal phase and cubic phase. The UV emission located at 398 nm disappears and the peak at 383 nm increases with further increasing temperature.

The existence of various defects related to zinc and oxygen is an important reason leading to the visible emission. According to Sun's calculation by using full-potential linear muffin-tin orbital (FP-LMTO) method [25], the blue emission located at 427 nm may be caused by the electronic transition between the donor level of Zn interstitial (Zn_i) and valence band. The emission peak

located at 489 nm is most likely to be caused by the electronic transition between the shallow conduction band level and acceptor level of anti-oxygen (O_{Zn}) [2]. It is observed from the PL spectrum that the best luminescence behavior is shown for the film fabricated at 600°C. Study shows that the PL properties of thin films are more dependent on the stoichiometry than that of the crystal quality [26]. Experimental results are further evidences that the temperature of 400°C is the most appropriate in the preparation of ZnMgO thin films with good crystalline structure, and the film fabricated at 600°C with better stoichiometry possesses the best luminescence property.

4 Conclusion

ZnMgO thin films were fabricated on Si(111) substrates at the temperature from 300 to 700°C by PLD technique. XRD show that the best thin film with high crystallinity and high c-axis preferred orientation is obtained at growth temperature of 400°C. With the increase of growth temperature, a transformation of the ZnMgO crystal structure from hexagonal wurtzite to rock-salt-cubic structure is observed, indicating the Magnesium compositions in the films is increased. The PL spectra reveal that the UV emission intensity of ZnMgO thin films increases with increasing growth temperature and the film with the best photoluminescence property is obtained at 600°C. The blue-shift from 398 to 383 nm of the UV emission for the ZnMgO films fabricated from 300 to 700°C is observed, which is attributed to the increase of the band-gap of ZnMgO structure from 2.96 to 4.23 eV due to the increasing Mg content.

Acknowledgments The authors are grateful for the financial support by the Provincial Natural Science Foundation of Shandong (Y2008A21, ZR2009FZ006,ZR2010EL017), the Doctor Foundation of University of Jinan (XBS0833), and the Provincial Science and Technology Project of Shandong (2009GG20003028).

References

1. H. Natsuhara, K. Matsumoto, N. Yoshida, T. Itoh, S. Nonomura, M. Fukawa, K. Sato, Sol. Energ. Mater. Sol. Cell. **90**, 2867 (2006)
2. X.Q. Wei, J.Z. Huang, M.Y. Zhang, Y. Du, B.Y. Man, Mater. Sci. Eng. B **166**, 141–146 (2010)
3. K. Ajay, K. Davinder, Sol. Energ. Mater. Sol. Cell. **93**, 193 (2009)
4. D.K. Hwang, M.C. Jeong, J.M. Myoung, Appl. Surf. Sci. **225**, 217 (2004)
5. S. Choopun, R.D. Vispute, W. Yang, R.P. Sharma, T. Venkatesan, H. Shen, Appl. Phys. Lett. **80**, 1529 (2002)
6. A. Ohtomo, M. Kawasaki, T. Koida, K. Masubuchi, H. Koinuma, Y. Sakurai, Y. Yoshida, T. Yasuda, Y. Segawa, Appl. Phys. Lett. **72**, 2466 (1998)
7. A. Ohtomo, M. Kawasaki, Y. Sakurai, I. Ohkubo, R. Shiroki, Y. Yoshida, T. Yasuda, Y. Segawa, H. Koinuma, Mater. Sci. Eng. B **56**, 263 (1998)
8. W.I. Park, G.C. Yi, H.M. Jang, Appl. Phys. Lett. **79**, 2022 (2001)
9. R. Ghosh, D. Basak, Appl. Surf. Sci. **255**, 7238 (2009)
10. Y. Ramin, J.S. Farid, R.M. Muhamad, A. Mahendra, Solid State Sci. **12**, 1088 (2010)
11. J.P. Kar, M.C. Jeong, W.K. Lee, J.M. Myoung, Mater. Sci. Eng. B **147**, 74–78 (2008)
12. I. Hayashi, M.B. Panish, P.W. Foy, S. Sumski, Appl. Phys. Lett. **17**, 109 (1970)
13. W.I. Park, J. Yoo, D.W. Kim, G.C. Yi, M. Kim, J. Phys. Chem. B **110**, 1516 (2006)
14. R.K. Sahu, M.L. Rao, S.S. Manoharan, J. Mater. Sci. **36**, 4099 (2002)
15. Z.Q. Chen, G.J. Fang, C. Li, S. Sheng, G.W. Jie, X.Z. Zhao, Appl. Surf. Sci. **252**, 8657 (2006)
16. B.E. Warren, *X-ray Diffraction* (Dover, New York, 1990), p. 253
17. A. Kumar, P. Singh, D. Kaur, J. Jesudasan, P. Raychaudhuri, Appl. Phys. **39**, 5310 (2006)
18. J.Y. Zhang, D.Y. Jiang, Z.G. Ju, D.Z. Shen, B. Yao, X.W. Fan, Chin. J. Opt. Appl. Opt. **1**, 80 (2008)
19. W. Yuan, L.P. Zhu, Z.Z. Ye, X.Q. Gu, Appl. Surf. Sci. **256**, 1452 (2009)
20. M. Arivanandhan, K. Sankaranarayanan, K. Ramamoorthy, Cryst. Res. Technol. **39**, 692 (2004)
21. X. An, H.Z. Zhuang, L. Yang, C.S. Xue, Appl. Surf. Sci. **193**, 87 (2002)
22. N. Laidani, R. Capelletti, M. Elena, L. Guzman, G. Mariotto, A. Miotello, P.M. Ossi, Thin Solid Films **223**, 114 (1993)
23. M. Liu, X.Q. Wei, Z.G. Zhang, G. Sun, C.S. Chen, C.S. Xue, H.Z. Zhuang, B.Y. Man, Appl. Surf. Sci. **252**, 4321 (2006)
24. D.C. Look, D.C. Reynolds, J.R. Sizelove, R.L. Jones, C.W. Litton, G. Cantwell, W.C. Harsch, Solid State Commun. **105**, 399 (1998)
25. B. Lin, Z. Fu, Y. Jia, Appl. Phys. Lett. **79**, 943 (2001)
26. X.Q. Wei, B.Y. Man, C.S. Xue, C.S. Chen, M. Liu, Jpn. J. Appl. Phys. **11**, 8586 (2006)